JOINT INSTITUTE FOR NUCLEAR RESEARCH
Bogoliubov Laboratory of Theoretical Physics

FINAL REPORT ON THE

START PROGRAMME

Wavelet analysis of giant monopole resonance in light nuclei

Supervisor:
Dr. Valentin Olegovich Nesterenko

Student:
Nikita Andreevich Ashurko, Russia
Tomsk State University

Participation period:
July 21 – August 31,
Summer Session 2024

Dubna, 2024

ABSTRACT

The report "Wavelet analysis of giant monopole resonance in light nuclei" consists of 15 pages of the text, 7 figures, 3 tables, and the reference list with 16 citations.

Keywords: giant monopole resonance, deformation-induced coupling of monopole and quadrupole modes, fine structure, Landau damping, Skyrme energy density functional, self-consistent quasiparticle random-phase approximation, wavelet analysis, reaction (α, α'), ^{24}Mg.

The object of this study are E0 states in ^{24}Mg.

The main objective of this work: To perform the comparative wavelet analysis of theoretical and experimental data for E0 excitations in the regions of monopole-quadrupole coupling (MQC) and monopole giant resonance (GMR) and determine dominant widths (scales) characterising fine structure of E0 spectra to clarify the role of different decay mechanisms.

Research methods: iThemba experiment (α, α') for ^{24}Mg, Quasiparticle random-phase approximation (QRPA) method with Skyrme forces, continuous wavelet transform with Morlet mother function, wavelet scales and powers.

In the work, the wavelet analysis of E0 excitations in deformed nucleus ^{24}Mg was performed. The MQC and GMR regions were investigated. We used iThemba (α, α') experimental data and our QRPA results. The experimental and theoretical wavelet transforms and powers for theoretical and experimental data were compared and characteristic widths (scales) were determined. Besides, to clarify the role of the residual interaction, the QRPA wavelet results were compared with unperturbed two-quasiparticle (2qp) ones. Thus the dominant role of the Landau damping in fine structure of E0 excitations in light deformed nuclei was demonstrated.

OVERVIEW

1 Introduction 3
2 Calculation scheme 4
3 Monopole-quadrupole coupling in ^{24}Mg: experiment vs theory 5
4 Basics of wavelet analysis 6
5 Results and discussion 7
6 Conclusions 14
References 14

1 Introduction

Despite a long previous experimental and theoretical effort, investigation of giant resonances (GR) remains to be very actual [1, 2, 3, 4]. Giant resonances represent a valuable source of information on various nuclear properties including nuclear matter. Besides, GR are a robust test for modern self-consistent theoretical methods based on the energy density functional (EDF) theory. The E0 monopole giant resonance (GMR) is especially important since it provides the important information on the nuclear incompressibility [1].

GR are collective excitations of nuclei, exhausting the major part of the corresponding sum rules. They manifest themselves as powerful and broad maxima dominating in the cross sections of reactions of nuclei with various particles and external fields [1].

One of the main GR properties is its width Γ_{GR} [1]. The width is the result of various decay processes of GR. It usually has typical values of a few MeV. The total GR width can re roughly separated into three parts:

$$\Gamma_{GR} = \Delta\Gamma + \Gamma^{\uparrow} + \Gamma^{\downarrow} \tag{1}$$

where $\Delta\Gamma$ – the Landau damping describing a fragmentation of the collective mode to nearby elementary one-particle-hole (1p-1h) excitations, $\Gamma^{\uparrow}$ – the escape width, corresponding to the direct emission of particles from the continuum, and $\Gamma^{\downarrow}$ – the propagation width due to coupling to two-particle-two-hole (2p-2h) and multi-particle-small-hole (np-nh) states. Information about the dominant damping mechanisms of nuclear GR can be found in the properties and characteristics of the fine structure of the resonances. This fine structure is caused by the mixing of several scales of fluctuations that are induced by the decay of nuclear states.

In spherical nuclei, the coupling with complex configurations results in the significant (sometime decisive) role of $\Gamma^{\downarrow}$, see e.g. studies for the giant quadrupole resonance (GQR) [5, 6] and GMR [7]. Instead, in deformed nuclei, the GMR width is mainly provided by the Landau damping [4]. Besides, in deformed nuclei there is a remarkable coupling of isoscalar monopole and quadrupole (K=0) modes [4]. This monopole-quadruppole couling (MQC) leads to additional structures just below the main GMR [4]. Actually, in deformed nuclei, IS GMR and GQR must be described simultaneously. Narrow IS peaks induced by deformation-induced E0/E2 coupling can serve as an additional sensitive measure of nuclear incompressibility [8].

One of the most optimal methods to analyze fine structure and widths is the wavelet analysis [5, 6]. Wavelet is a mathematical function that allows you to analyze various frequency components of data. The graph of the function looks like a wave-like oscillation with amplitude decreasing to zero far from the origin. Wavelet analysis is used in tasks related to the analysis of spatial fields with complex multiscale structure or temporal signals with spectral composition changing with time (seismic signals). The main idea is to use a basis, each function of which characterizes both a certain spatial (temporal) frequency and

the place of its localization in physical space (time).

In this study, we describe E0 excitations in ^{24}Mg within the quasiparticle random phase approximation (QRPA) with Skyrme forces. The wavelet analysis is used to analyze fine structure of the experimental iThemba data and the theoretical strength functions in deformed nucleus ^{24}Mg. By comparison of 2qp and QRPA results we investigate the role of the Landau damping. Besides, we compare the wavelet results for energy regions of MQC and GMR.

2 Calculation scheme

The calculations were carried out within the QRPA model [11] based on the Skyrme functional. The model is fully self-consistent. Both the mean field and the residual interaction are obtained from the original Skyrme functional. The residual interaction takes into account all terms derived from the Skyrme functional and the Coulomb (direct and exchange) parts. Particle-hole and particle-particle [11] channels are included. The pairing interaction is considered at the BCS level [11].

The Hamiltonian

$$H = H_{mf} + H_{pair} + H_{res} \tag{2}$$

includes mean field part H_{mf}, pairing contribution H_{pair} and residual interaction H_{res}.

Skyrme parametrizations SkP$^{\delta}$ [12] and SVbas [13] are used. They give essentially different modulus of nuclear incompressibility: K_{∞} =202 and 234 MeV, respectively. SV-bas has a large (though rather typical for Skyrm forces) incompressibility but poorly describes IS GMR experimental data for light nuclei [8]. Instead, SkP$^{\delta}$ with its very low incompressibility demonstrates much better performance [8].

Both parametrizations were earlier applied for description of GMR in ^{24}Mg and ^{28}Si [7]. SV-bas has a large (though rather typical for Skyrm forces) incompressibility.

A large configuration space is used in the calculations. The single-particle spectrum extends from the bottom of the potential well to 30 MeV. The two-quasiparticle (2qp) basis in QRPA calculations with SkP$^{\delta}$ extends to 70 MeV. The QRPA isoscalar monopole (L=0) and quadrupole (L=2) transition strengths are presented in terms of strength functions

$$S_L(E) = \sum_{K=0}^{L}(2-\delta_{K,0}) \sum_{\nu\in K} |\left\langle \nu|\hat{O}_{LK}|0\right\rangle|^2 \xi_{\Delta}(E-E_{\nu}) \tag{3}$$

where ν denotes the QRPA excitation state $|\nu\rangle$ with energy E_{ν} and $|0\rangle$ isthe ground QRPA state. The monopole and quadrupole isoscalar transition operators are $\hat{O}_{00} = \sum_i^A r_i^2$ and $\hat{O}_{20} = \sum_i^A r_i^2 Y_{20}(\hat{r}_i)$, respectively. For convenience of comparison with experimental data, the strength is smoothed by the Lorentzian function $\xi_{\Delta}(E-E_{\nu}) = \Delta/(2\pi[(E-E_{\nu})^2 - \Delta^2/4])$ with averaging parameter Δ = 100 keV. The energy E is considered as the array with the grid step ΔE=20 keV. The dimension of the strength functions is fm^4/MeV. We also present the 2qp force functions calculated without considering the residual interaction. In this case,

the number ν in the equation (3) denotes 2qp states.

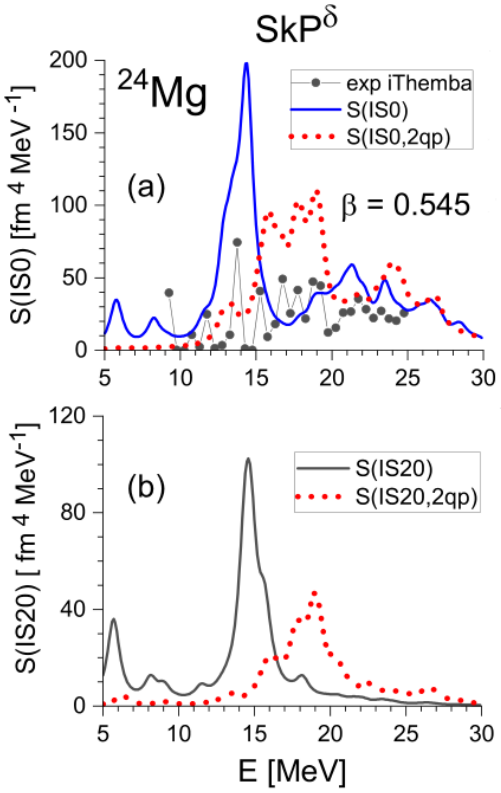

Figure 1 — Top panels: IS0 QRPA (solid blue line) and 2qp (short dashed red line) strength functions calculated with the SkP strength (K_{∞}=202 MeV) in ^{24}Mg are compared with the current iThemba LABS experimental data, shown as black filled circles. Bottom panels: QRPA (solid black line) and 2qp (short dashed red line) of IS20 strength [8]

3 Monopole-quadrupole coupling in ^{24}Mg: experiment vs theory

The experiment [8] was carried out in the iThemba LABS laboratory, South Africa. A beam of α-particles was inelastically scattered on a self-supported ^{24}Mg-target. After extraction of the inelastic scattering cross sections, isoscalar monopole (IS0) strength distribution was obtained using the difference-of-spectra (DoS) method with excitation energy dependent corrections.

In Fig.1, the MQC effect in ^{24}Mg is demonstrated using Skyrme force SkP$^{\delta}$ [8]. In the upper panel of the figure, the QRPA IS0 monopole strength functions from the equation (3) are compared with the experimental data. The iThemba LABS experimental data are shown as black filled circles, where each data point accumulates the IS0 strength in the 0.5 MeV energy range. Fig.1 shows that both experimental and QRPA IS0 strengths segregate into a narrow structure at ≈15 MeV in ^{24}Mg and a broad structure at higher energies, which is a typical picture for deformed nuclei. The comparison of IS0 and IS2(K=0) strengths shows that IS0 peak arises just due to MQC effect. It is also useful to compare the QRPA IS0 strength with the 2qp IS0 strength (red dashed line) obtained without residual interaction. We see a strong collective effect: the residual interaction significantly shifts down the IS0

strength and creates collective peaks at ≈15 MeV in ^{24}Mg.

4 Basics of wavelet analysis

In this report, wavelet analysis based on the continuous wavelet transform (CWT) is used for scale extraction [15].

The wavelet analysis can be roughly treated as a local Fourier transformation. The wavelet transform $C(\delta E, E_x)$ (usually complex-valued) of some signal $\sigma(E)$ is defined as a convolution of the signal with a particular mother wavelet function Ψ:

$$C(\delta E, E_x) = \frac{1}{\sqrt{\delta E}} \int \sigma(E) \Psi^* \left(\frac{E_x - E}{\delta E} \right) dE \tag{4}$$

The parameter δE scales, i.e., expands or stretches, the function, and the parameter E_x shifts the wavelet position along the excitation energy so that information about the localization of the scale becomes available. This transformation results in a two-dimensional (2D) distribution of wavelet coefficients $C(\delta E, E_x)$. These coefficients will be large at those scales δE and locations E_x where the shape of the scaled and shifted wavelet $\Psi(x)$ has the greatest similarity to the analyzed data sample $\sigma(E)$. Instead, if the scale of the wavelet function is very different from the characteristic scales at this location, the coefficients will be small. Consequently, if we study this two-dimensional distribution of wavelet coefficients, we can extract not only the values of characteristic scales, but also their locations, which is very important for the thorough analysis.

Another important advantage of wavelet analysis is the ability to use different wavelet mother functions most suitable for a particular problem, thus extracting the necessary features in the most efficient way. In order to obtain the desired representation of a signal using wavelet analysis, it is necessary to select the function that best resembles the features of the signal under study. The shape of the wavelet function should be similar to the shape of the signal, but the scaling resolution of different wavelets should also be taken into account. It was shown by Shevchenko et al [5] that the Morlet wavelet function is most suitable for analysis of fine structure of GR.

The Morlet function is obtained by taking a periodic wave and localizing it with a Gaussian envelope that is superimposed on a sinusoidal structure [16],

$$\Psi_{Morlet}(x) = \pi^{-1/4} e^{ikx} e^{-x^2/2} \tag{5}$$

where k defines the number of sinusoidal oscillations in the Gaussian window. Strictly speaking, the Morlet function (5) is not applicable as a wavelet because it does not satisfy the admissibility condition (6). However, k can be chosen such that $\Psi(0)$ is close to zero. Hence, we must choose a value of k large enough to hold, at least approximately, the condition $\Psi(0) = 0$. For this purpose $k \geq 5$ is suitable, then the quadratic integrability condition is

satisfied [16],

$$K_\Psi = \int_{-\infty}^{\infty} |\Psi^2(x)|dx < \infty \tag{6}$$

is satisfied within the accuracy of calculations with single-precision arithmetic. Higher values of k will slightly improve the scale resolution, and in the limiting case we obtain the Fourier spectrum. For the analysis of the nuclear giant resonance spectra described below, a value of $k = 5$, provides the best value [6].

It is convenient to extract the dominant widths (energy scales δE) using so-called wavelet powers

$$P(\delta E) = \frac{1}{N} \sum_i |C_i(\delta E, E_x(i))C_i^*(\delta E, E_x(i))| \tag{7}$$

where $i = 1, ..., N$ runs all the energy grid range (N is the number of energy bins in the considered excitation-energy range).

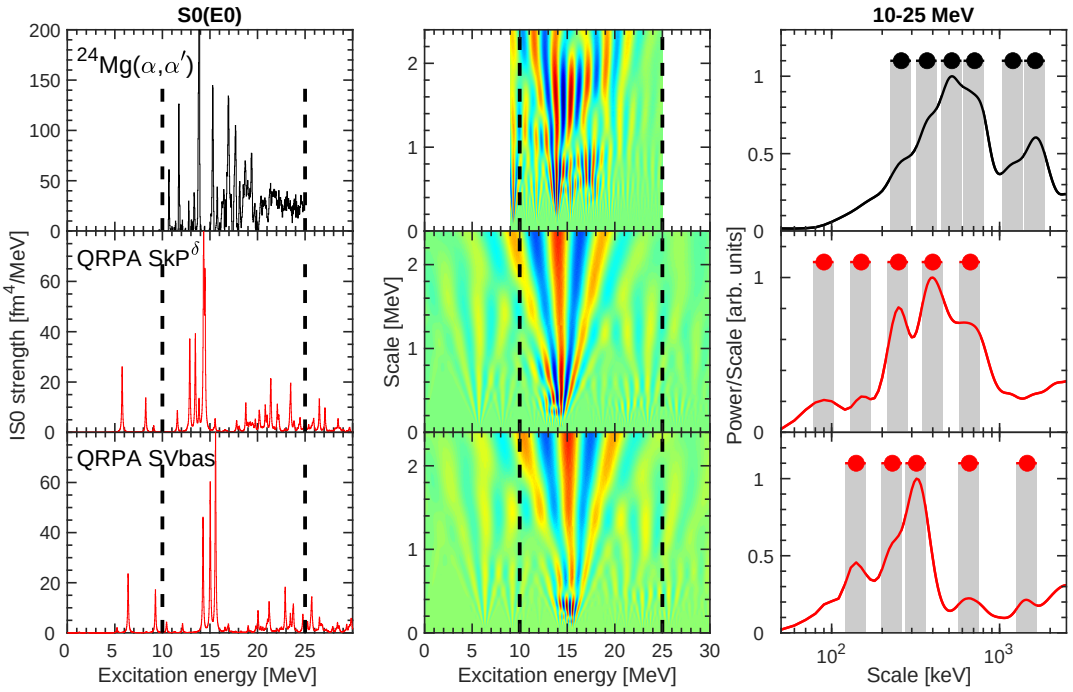

Figure 2 — Experimental and theoretical IS0 strength functions for ^{24}Mg (left), corresponding squared wavelet transforms $C(\delta E, E_x) * C^*(\delta E, E_x)$ (middle) and wavelet powers (right). The powers are estimated for the energy region indicated by the vertical dashed lines (10 MeV $\leq E_x \leq$ 25 MeV) in the left panel. The black and red dots mark the dominant (characteristic) scales δE)

5 Results and discussion

Fig.2 shows IS0 experimental and theoretical (SkP$^\delta$, SV-bas) strength functions in ^{24}Mg and corresponding wavelet transforms and powers. The energy range 10 MeV $\leq E_x \leq$ 25 MeV covers both MQC and GMR regions. The red and blue shades in the middle panels

serve as a measure of magnitudes of squared wavelet transforms $C(\delta E, E_x) * C^*(\delta E, E_x)$. The specific pattern of alternating regions of large and small coefficients as a function of E_x is due to the use of an oscillating function. For extraction of the scales dominating in the considered energy region, it is convenient to consider wavelet powers (right panels). The maxima of the power spectrum are treated as characteristic scales of distribution of IS0 strength in ^{24}Mg. Since power values generally grow with the scale, the scale axis in Fig.2 is limited to 2 MeV for a better visibility of the characteristic scales at lower energies.

Left panels of Fig.2 show that SkP$^\delta$ well reproduces the experimental strength distribution. Besides, SkP$^\delta$ provides a reasonable agreement for the squared wavelet transforms (middle panels) and gives a nice description of wavelet powers (right panels). SV-bas results are much worse.

Experimental and SkP$^\delta$ powers in Fig.2 show that the most dominant scales are concentrated at 0.2 MeV $< \delta E <$ 1 MeV. Following previous studies [5, 6], the characteristic scales scales can be divided into three groups: small scales around 100 keV, medium scales at 100 keV — 1 MeV and large scales of the order of several MeV. The scales from these three groups, extracted from Fig.2, are collected in Table 1. It is seen that, at least for the medium scales, we have a reasonable agreement with the experiment.

Table 1 — Summary of the characteristic scales deduced from the CWT analysis for the energy interval 10-25 MeV

Dataset	Scales (keV)		
	Small	Medium	Large
Expt.		260, 370, 520, 710	1200, 1630
SkP$^\delta$	90	150, 250, 400, 670	
SVbas		140, 230, 320, 660	1460

To inspect the impact of the monopole-quadrupole coupling, let's now perform the similar analysis for MQC energy region (10 MeV $\leq E_x \leq$ 15 MeV). Following Fig.3, SLy6 results are again in rather good agreement with thee experiment. Again the powers demonstrate that most dominant widths lie in the range 0.2 MeV — 1 MeV. The total set of the characteristic widths is exhibited in Table 2. For medium scales we have rather good agreement with the experiment.

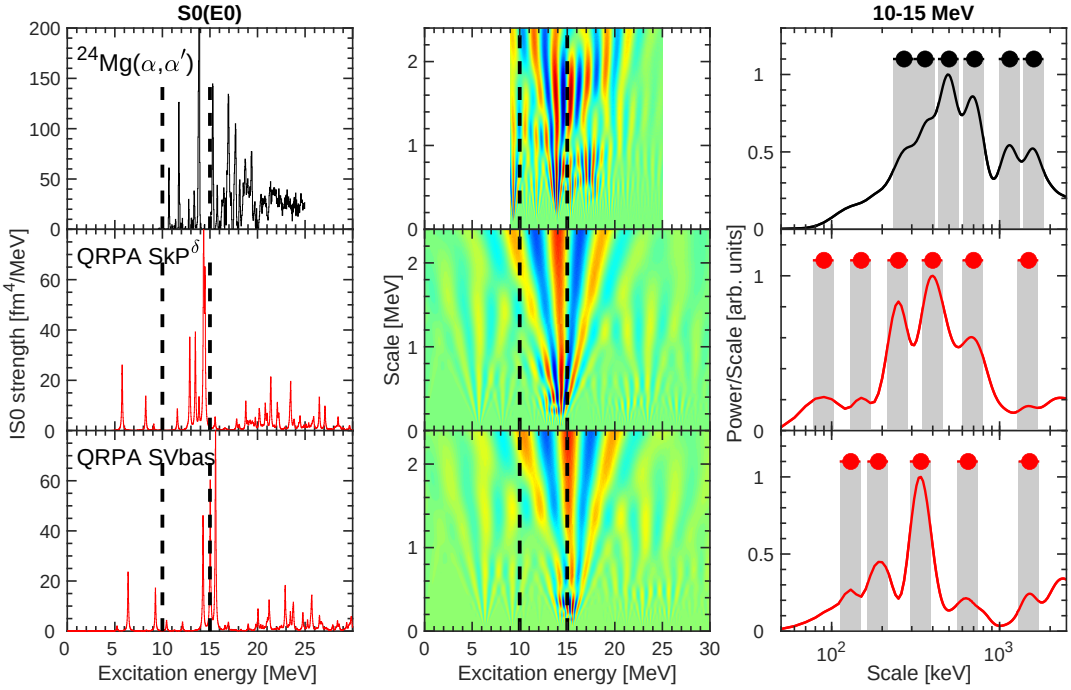

Figure 3 — The same as in Fig. 2 but now for MQC energy range (10 MeV $\leq E_x \leq$ 15 MeV) indicated in the left panels

Table 2 — Summary of the characteristic scales deduced from the CWT analysis (in keV) for the energy interval 10-15 MeV

Dataset	Scales (keV)		
	Small	Medium	Large
Expt.		270, 360, 500, 710,	1150, 1600
SkP$^{\delta}$	90	150, 250, 400, 700	1490
SVbas		130, 190, 340, 650	1510

The results for GMR energy region (15 MeV $\leq E_x \leq$ 25 MeV) are shown in Fig. 4 and Table 3. The results look similar to those for MQC energy range (10 MeV $\leq E_x \leq$ 15 MeV) (though with more medium scales in ther GMR case).

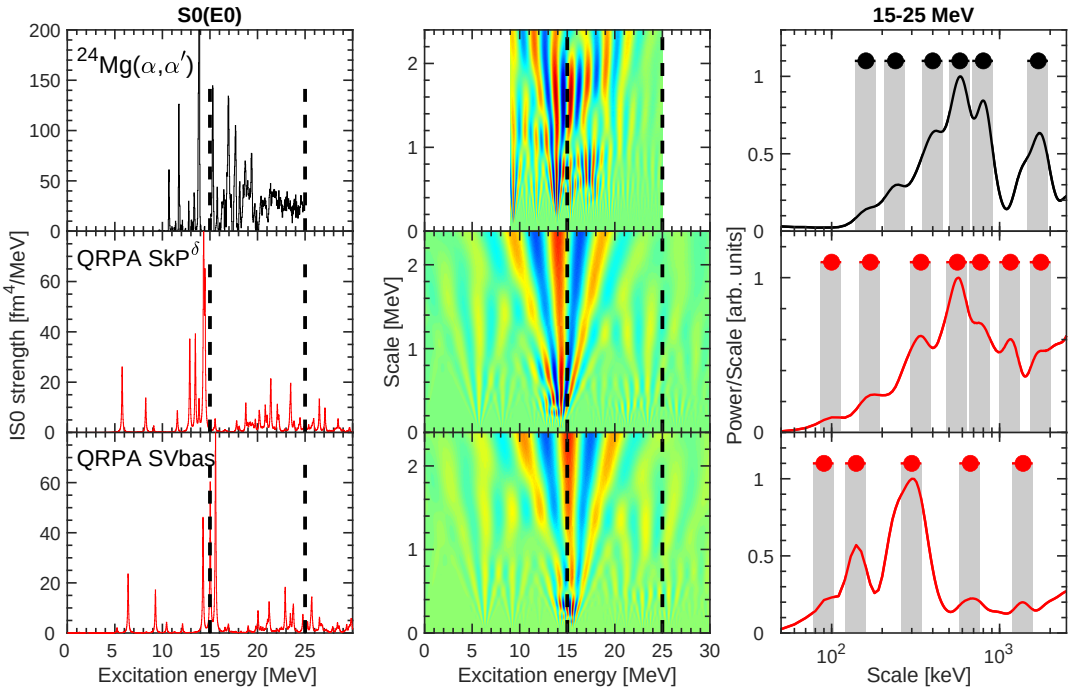

Figure 4 — The same as in Fig. 2 but now for GMR energy range 15 MeV $\leq E_x \leq$ 25 MeV

Table 3 — Summary of the characteristic scales deduced from the CWT analysis (in keV) for the energy interval 15-25 MeV

Dataset	Scales (keV)		
	Small	Averages	Large
Expt.		160, 240, 400, 580, 800	1700
SkP$^{\delta}$	100	170, 340, 560, 770	1160, 1760
SVbas	90	140, 300, 670	1380

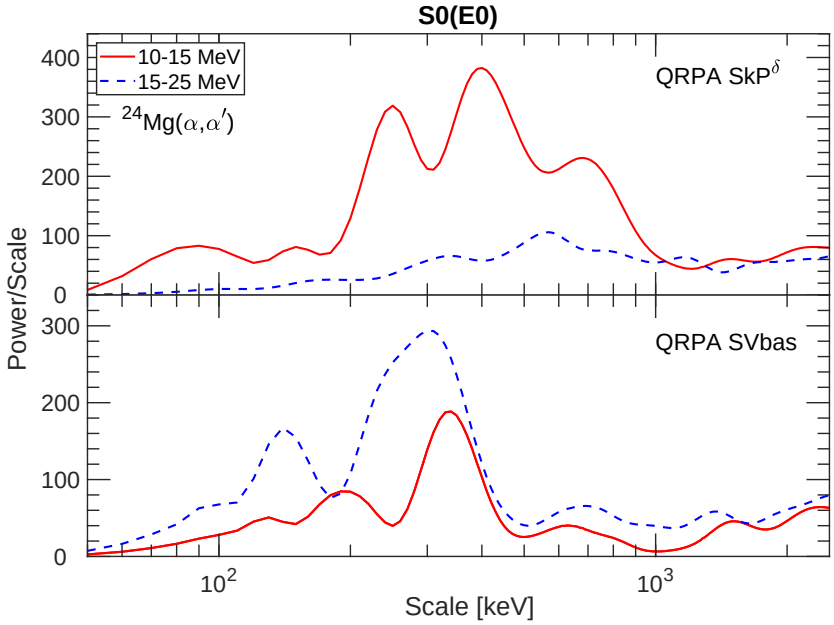

Figure 5 — Comparison of non-normalized SkP$^{\delta}$ (top) and SV-bas (bottom) powers for energy intervals 10-15 MeV and 15-25 MeV.

Note that the apparent similarity of the powers in MQC and GMR cases is actually somewhat misleading because we use in Figs. 3 and 4 the normalized powers. In this connection, it is worth to consider the powers without the norminalisation. This is done in Fig.5. This figure shows a strong dominance of MQC contribution for SkP$^{\delta}$ and of GMR contribution for SV-bas. As can be seen from Figs. 3 and 4, the difference in SkP$^{\delta}$ and SV-bas results can be trivially explained by the non-optimal choice of the boarder between MQC and GMR regions in SV-bas case. It is seen that some strong MQC peaks turned out to lie in the GMR range. So, just SkP$^{\delta}$ results in Fig.5 should be considered as relevant.

To clarify the impact of the residual interaction and role of Landau damping, it is instructive to compare QRPA results with unperturbed two-quasiparticle (2qp) ones obtained without the residual interaction. The theoretical results for 2qp strengths are exhibited in Fig.6. The left panels of the figure show that 2qp strength is upshifted as compared to QRPA strength. Following right panels, 2qp strength leads to a broader and more uniform distribution of the widths which vary from 0.1 to 2 MeV. As compared to QRPA case, the relative contribution of small widths grows. The 2qp characteristic scales, denoted in the figure by red dots significantly deviate from experiment and QRPA results.

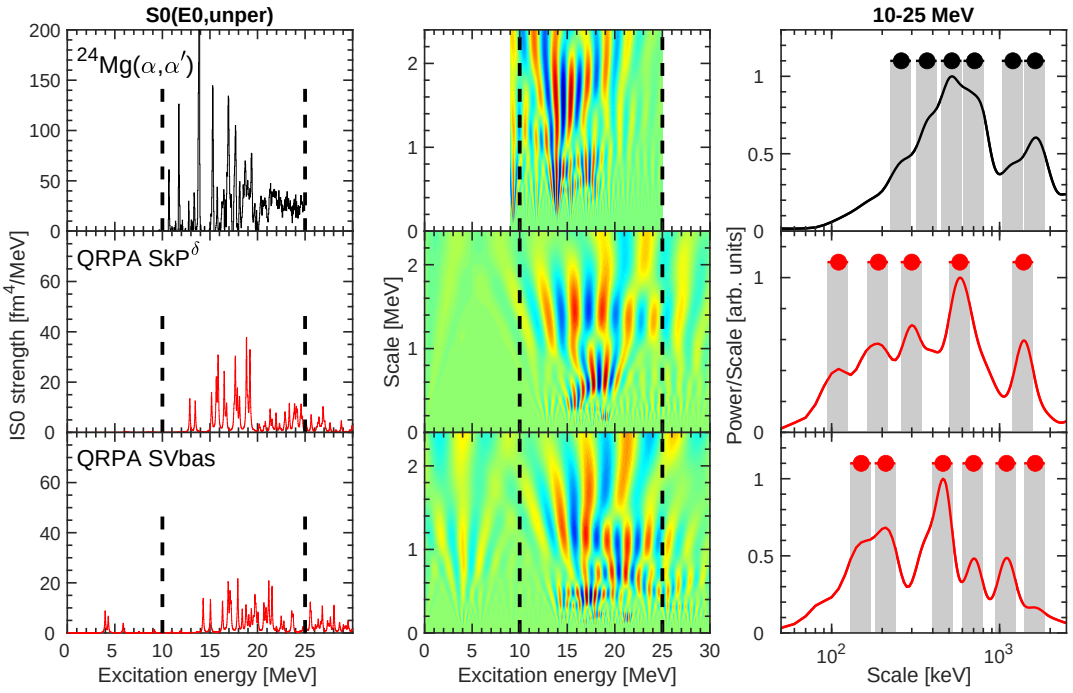

Figure 6 — The same as in Fig.2 but for 2qp theoretical strength.

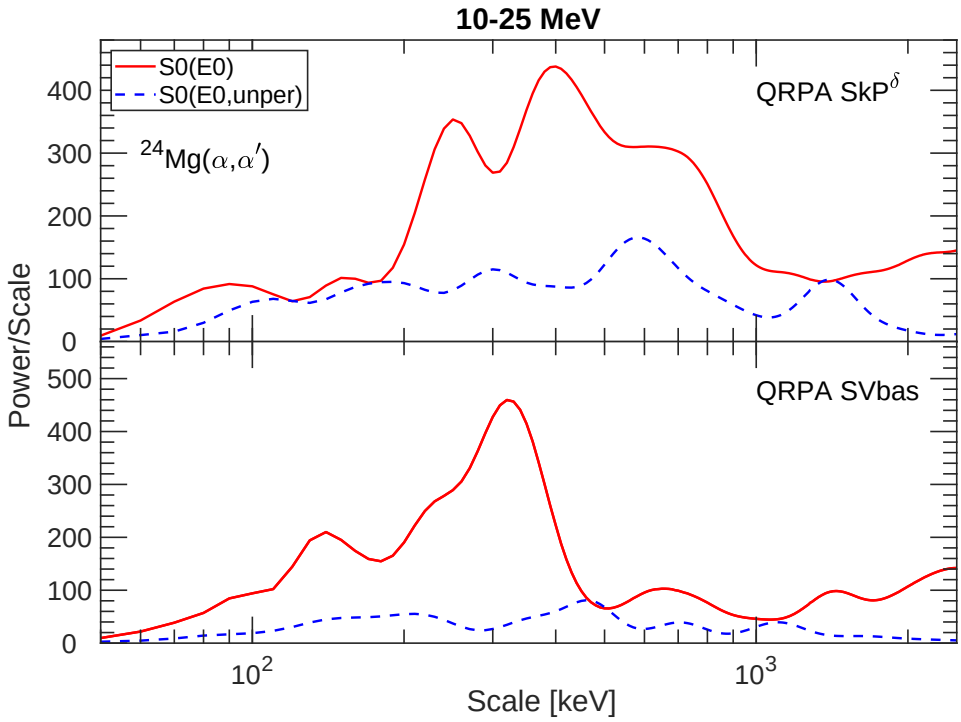

Figure 7 — Comparison of Skp$^{\delta}$ and SV-bas powers obtained with and without the residual interaction.

The non-normalized SkP$^{\delta}$ and SV-bas powers obtained with and without the residual interaction are compared in Fig.7. We see that 2qp strength leads to a broad and rather uniform distribution of the widths. The residual interaction redistributes the widths in favor of medium widths 0.2 - 1 MeV. Just these medium widths mainly represent the Landau damping. Altogether, we see very important role of the residual interaction. The maximum QRPA peaks are 3 times higher than in the unperturbed case. Thus, the dominant role of Landau damping in the fine structure of E0-excitations in light deformed nuclei is demonstrated.

6 Conclusions

In this report, a comparative wavelet analysis of theoretical and experimental data has been performed for E0 excitations in the deformed nucleus ^{24}Mg in the monopole-quadrupole coupling (MQC) and giant monopole resonance (GMR) regions. The theoretical results are obtained in the framework of QRPA method using Skyrme forces SkP$^{\delta}$ and SV-bas with nuclear incompressibility K_{∞} =202 and 234 MeV, respectively.

The following results are obtained:

1. The force SkP$^{\delta}$ with a low incompressibility well reproduces experimental strength functions, wavelet powers and characteristic widths (scales). The most dominant widths have values 0.2-1 MeV. The performance of the force SV-bas is essentially worse. So, Skyrme forces with a low incompressibility look preferable for description of E0 excitations in light deformedv nuclei.,

2. The separate wavelet analysis is done for monopole-quadrupole coupling (MQC) and giant monopole resonance (GMR) energy regions. The dominance of MQC powers is demonstrated.

3. The comparison of the QRPA and unperturbed 2qp wavelet results shows the dominant role of the residual interaction and Landau damping in the fine structure of E0-excitations. Just these factors resul in the proper strength functions and wavelet powers.

REFERENCES

[1] Harakeh M.N. Giant Resonances: Fundamental High-Frequency Modes of Nuclear Excitation / M. N. Harakeh and A. van der Woude // Oxford Studies in Nuclear Physics — 2001. — V. 24.

[2] Garg U. The compression-mode giant resonances and nuclear incompressibility / U. Garg and G. Colò // Prog. Part. Nucl. Phys. — 2018. — V. 101 — 55.

[3] Ishkhanov, B.S. Giant dipole resonance of atomic nuclei: the history of prediction, discovery, and study of a unique phenomenon. 75 years of research / B.S. Ishkhanov, I.M. Kapitanov // M.: LENAND, 2021. — 278 p.

[4] Kvasil J. Deformation-induced splitting of the isoscalar E0 giant resonance: Skyrme random-phase-approximation analysis / J. Kvasil, V.O. Nesterenko, A. Repko, W. Kleinig and P.-G. Reinhard // Physical Review C — 2016. — V. 94 — 064302.

[5] Shevchenko A. Analysis of fine structure in the nuclear continuum / A. Shevchenko, J. Carter, G.R.J. Cooper et al // Physical Review C — 2008. — V. 77 — 024302. doi: 10.1103/PhysRevC.77.024302.

[6] Shevchenko A. Global investigation of the fine structure of the isoscalar giant quadrupole resonance / A. Shevchenko, O. Burda, J. Carter et al // Physical Review C — 2009. — V. 79 — 044305. doi: 10.1103/PhysRevC.79.044305.

[7] Bahini A. Fine structure of the isoscalar giant monopole resonance in ^{58}Ni, ^{90}Zr, ^{120}Sn, and ^{208}Pb / A. Bahini, P. von Neumann-Cosel, J. Carter et al // Physical Review C — 2024. — V. 109 — 014325. doi: 10.1103/PhysRevC.109.014325.

[8] Bahini A. Isoscalar giant monopole resonance in ^{24}Mg and ^{28}Si: Effect of coupling between the isoscalar monopole and quadrupole strength / A. Bahini, V.O. Nesterenko, I.T. Usman et al // Physical Review C — 2022. — V. 105 — 024311. doi: 10.1103/PhysRevC.105.024311.

[9] Migdal A. Quadrupole and dipole γ-radiation // Journal of Experimental and Theoretical Physics — Vol. 15, № 3. — C. 81 — 88.

[10] Kureba C.O. Wavelet signatures of K-splitting of the Isoscalar Giant Quadrupole Resonance in deformed nuclei from high-resolution (p, p') scattering off ^{146,148,150}Nd / C.O. Kureba, Z. Buthelezi, J. Carter et al // Physics Letters B — 2018. — V. 779 — P. 269 — 274. doi: 10.1016/j.physletb.2018.02.013.

[11] A. Repko. Pairing and deformation effects in nuclear excitation spectra / A. Repko, J. Kvasil, V.O. Nesterenko and P.-G. Reinhard // Eur. Phys. J. A — 2017. — V. 53 — 221.

[12] Dobaczewski J. Closed shells at drip-line nuclei / J. Dobaczewski, W. Nazarewicz and T. R.Werner // Phys. Scr. — 1995. — V. 56 — 15. doi: 10.1088/0031-8949/1995/T56/002.

[13] Klupfel P. Variations on a theme by Skyrme: A systematic study of adjustments of model parameters / P. Klupfel, P.-G. Reinhard, T.J. Burvenich and J.A. Maruhn // Physical Review C — 2009. — V. 79 — 034310. doi: 10.1103/PhysRevC.79.034310.

[14] Stone J.R. The Skyrme interaction in finite nuclei and nuclear matter / J.R. Stonea, P.-G. Reinhard // Progress in Particle and Nuclear Physics — 2007. — V. 58 — P. 587—657.

[15] Daniel T.L. Wavelet Analysis: Theory and Applications / T.L. Daniel and Akio Yamamato // Hewlett-Packard Journal — 1994.

[16] Nirdosh Bhatnagar. Introduction to Wavelet Transforms // © 2020 by Taylor & Francis Group, LLC.